# ONE LR DOESN'T FIT ALL: HEAVY-TAIL GUIDED LAYERWISE LEARNING RATES FOR LLMS

**Di He**[1,2,3*], **Songjun Tu**[2,3*], **Keyu Wang**[4], **Lu Yin**[5], **Shiwei Liu**[6,7,8 †]
[1]Shenzhen Institutes of Advanced Technology, Chinese Academy of Sciences
[2]Peng Cheng Laboratory [3]University of Chinese Academy of Sciences
[4]University of Tübingen [5]University of Surrey
[6]Max Planck Institute for Intelligent Systems
[7]ELLIS Institute Tübingen [8]Tübingen AI Center
Correspondence to: sliu@tue.ellis.eu

## ABSTRACT

Learning rate configuration is a fundamental aspect of modern deep learning. The prevailing practice of applying a uniform learning rate across all layers overlooks the structural heterogeneity of Transformers, potentially limiting their effectiveness as the backbone of Large Language Models (LLMs). In this paper, we introduce **Layerwise Learning Rate (LLR)**, an adaptive scheme that assigns distinct learning rates to individual Transformer layers. Our method is grounded in Heavy-Tailed Self-Regularization (HT-SR) theory, which characterizes the empirical spectral density (ESD) of weight correlation matrices to quantify heavy-tailedness. Layers with weaker heavy-tailedness are assigned larger learning rates to accelerate their training, while layers with stronger heavy-tailedness receive smaller learning rates. By tailoring learning rates in this manner, `LLR` promotes balanced training across layers, leading to faster convergence and improved generalization. Extensive experiments across architectures (from LLaMA to GPT-nano), optimizers (AdamW and Muon), and parameter scales (60M–1B) demonstrate that `LLR` achieves up to 1.5× training speedup and outperforms baselines, notably raising average zero-shot accuracy from 47.09% to 49.02%. A key advantage of `LLR` is its low tuning overhead: it transfers nearly optimal LR settings directly from the uniform baseline. Code is available at https://github.com/hed-ucas/Layer-wise-Learning-Rate.

## 1 INTRODUCTION

Learning rate (LR) configuration is a cornerstone in modern deep learning, shaping both the convergence dynamics of training and the generalization ability of the resulting models (LeCun et al., 2015). Despite the rapid evolution of the LLM era—including the rise of Transformers (Vaswani et al., 2017), self-supervised learning (Radford et al., 2018), chain-of-thought reasoning (Wei et al., 2022), and RLHF (Ouyang et al., 2022)—the predominant LR strategy has remained essentially unchanged: applying a single LR value across all layers, which we refer to as the *Uniform LR*.

This paradigm, however, was originally developed for architectures with relatively homogeneous designs, such as multi-layer perceptrons (MLPs) and convolutional neural networks (CNNs). We contend that it does not adequately capture the structural heterogeneity of Transformer-based LLMs, thereby constraining their convergence and potentially their final performance. Specifically, recent studies highlight the **architectural heterogeneity** of Transformers, where the Hessian spectra differ substantially across layer types (Zhang et al., 2024a; Wang et al., 2025; He et al., 2025). These findings suggest that applying a single uniform LR might be inherently suboptimal, motivating the need for layerwise learning-rate strategies that explicitly account for such architectural heterogeneity in Transformer-based LLMs.

Research endeavors have explored the layerwise LR. For instance, the ratio between the weight norm and gradient norm of each layer has been used to set layerwise LRs, with the goal of stabilizing large-

[†]Corresponding author; * Equal contribution.

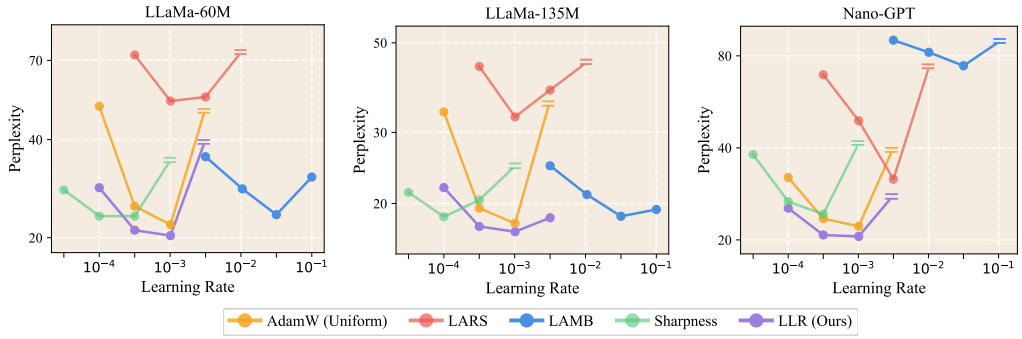


Figure 1: Learning rate sensitivity of different layerwise LR methods on LLaMa-60M, LLaMa-135M and Nano-GPT pre-training. Across all methods, data points failing to converge, resulting in excessively high perplexity values (exceeding the axis limits), are denoted by a **double dash ("=")**.

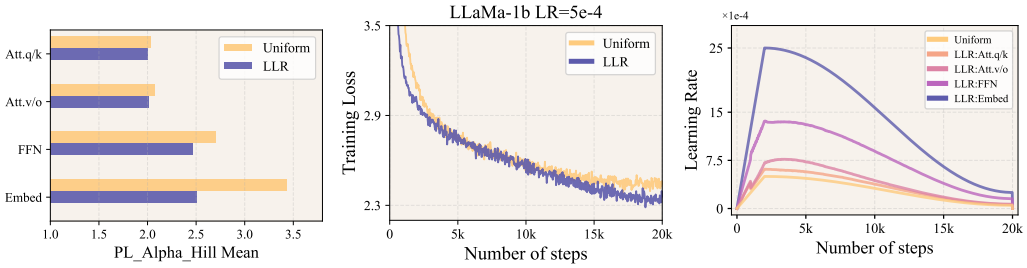


Figure 2: **Left:** Mean `PL_Alpha_Hill` value comparison (more balanced is preferred) between Uniform LR and LLR, with LLaMa-1B on FineWeb; **Middle:** Training loss curves under the AdamW optimizer; **Right:** Layerwise learning rate schedules when combining `LLR` with cosine decay scheduler. Performance comparison: `LLR` (Base LR=5e-4) obtains Perplexity (↓) =9.59 and Q-A Acc. (↑) =49.02%; `Uniform` (LR=5e-4) obtains Perplexity=9.77 and Acc.=47.09%, while `Uniform` (LR=2.5e-3) degrades to Perplexity=30.56.

batch training in CNNs (You et al., 2017) and BERT (You et al., 2019). More recently, Wang et al. (2025) identified sharpness disparities across Transformer modules and introduced a fixed layer-wise LR schedule determined via grid search. However, our preliminary evaluation in Figure 1 shows that these approaches are highly sensitive to LR tuning: their improvements emerge only when compared against the uniform baseline at its suboptimal LR, while they often underperform the uniform baseline when the latter is tuned to its optimal LR. This leaves an open research question: ***Does a principled layerwise LR scheme exist that can outperform the uniform LR even at its optimal LR?***

To this end, we propose **Layerwise Learning Rate (LLR)** for LLMs—an effective layerwise LR allocation strategy, grounded in Heavy-Tailed Self-Regularization (HT-SR) theory (Martin & Mahoney, 2019), that promotes balanced training across layers. `LLR` periodically measures the degree of heavy-tailedness in each layer's weight spectrum and assigns larger LRs to layers that are less heavy-tailed, while allocating smaller LRs to those exhibiting stronger heavy-tailedness. The underlying principle is drawn from HT-SR theory, which posits that layers with stronger heavy-tailedness are already better trained than those with weaker heavy-tailedness. Consequently, assigning larger LRs to the latter accelerates their training, thereby promoting more balanced progress across layers.

More concretely, `LLR` periodically computes the Empirical Spectral Density (ESD) across all layers, performs Power-Law (PL) fitting, and updates the corresponding `PL_Alpha_Hill` metrics. Layers with higher `PL_Alpha_Hill` values—typically embedding and FFN components—are assigned proportionally larger LRs, whereas layers with lower `PL_Alpha_Hill` values—such as attention modules—receive smaller LRs. This metric-to-map allocation scheme enables adaptive layerwise LR adjustment directly driven by spectral statistics, ensuring robust performance gains without extra hyperparameter-tuning burden. Our main contributions are as follows:

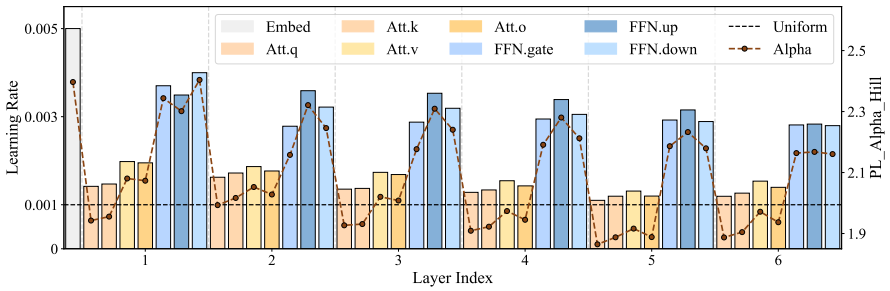


Figure 3: The bars denote the Learning Rate, and the line indicates the `PL_Alpha_Hill`. Given the imbalanced layerwise `PL_Alpha_Hill` of LLaMa-60M, `LLR` assigns lower LR to layers with lower `PL_Alpha_Hill`.

❶ We propose Layerwise Learning Rate (LLR), grounded by HT-SR theory, which enables dynamic assignment of LRs across layers within LLMs during training, promoting balanced training across layers.

❷ Extensive experiments on various architectures, including LLaMA (Table 2) to GPT-nano (Table 8), optimizers with AdamW and Muon, under Chinchilla scaling law from 60M to 1B, show that `LLR` yields up to a 1.5× training speedup (Figure 6). Under the same training token budget, `LLR` further surpasses existing layerwise approaches by a clear margin (Table 2 and Table 3).

❸ A key advantage of `LLR` is its low tuning overhead: it inherits nearly optimal LR settings directly from the standard uniform LR (Figure 1), thereby lowering the practical barrier to adoption.

## 2 METHODOLOGY

In this section, we revisit the HT-SR theory and outline the key metrics that underpin our analytical framework. Subsequently, we investigate the spectral characteristics of weights in LLM pretraining tasks, and, informed by these findings, we introduce the `LLR` algorithm, which utilizes the HT-SR theory to deliver substantial improvements in pretraining performance.

### 2.1 HT-SR THEORY

The HT-SR framework offers a systematic approach to characterizing the ESD of weight matrices in neural networks. Observations from prior work indicate that well-trained models tend to display ESDs with pronounced heavy-tails which is closely linked to higher training quality. Several studies have further revealed that, in LLMs, parameters that are well-optimized and those insufficiently trained can coexist throughout the entire training process, and such heterogeneity can significantly affect overall model performance (Zhou et al., 2023; He et al., 2025; Lu et al., 2024). Building upon this theoretical basis, we employ the HT-SR metric to measure the degree of spectral tail heaviness, applying lower LRs to layers with pronounced heavy-tail characteristics (e.g., `Att.q`, `Att.k`) and higher LRs to those with weaker heavy-tails (e.g., `FFN components`, `Embedding`), thereby promoting balanced optimization across layers to enhance generalization and overall effectiveness (see Figure 2). The extent of heavy-tailedness is determined quantitatively by fitting a power law (PL) to the ESD and using the resulting PL exponent ($\alpha$) as the measurement criterion.

We consider a network comprising $N$ layers, each associated with a weight matrix $\{W_l\}_{l=1}^{L}$ of shape $n \times m$ ($n \leq m$). For each layer, the ESD is computed from the eigenvalues of the correlation matrix $X_l = W_l^\top W_l$. Formally, the ESD is defined as $\text{ESD}(x) = \frac{1}{N}\sum_{i=1}^{N} \delta(x - \sigma_i)$, where $\delta(\cdot)$ denotes the Dirac delta function and $\sigma_i$ are the singular values. We model the ESD by PL distribution:

$$p(\lambda) \propto \lambda^{-\alpha}, \lambda_{\text{min}} < \lambda < \lambda_{\text{max}} \tag{1}$$

where $p(\lambda)$ represents the eigenvalue density within the specified range, and $\alpha$ serves as a quantitative measure of the heavy-tailedness of the spectrum. We visualize the ESD distributions and the corresponding PL fits in Figure 11 of Appendix E. The PL exponent $\alpha$ is estimated using the Hill estimator (Zhou et al., 2023; Liu et al., 2024). Let $\{\lambda_i\}_{i=1}^{n}$ denote the eigenvalues sorted in ascending order. The Hill estimator is given by:

$$\texttt{PL\_Alpha\_Hill} = 1 + \frac{k}{\sum_{i=1}^{k} ln\frac{\lambda_{n-i+1}}{\lambda_{n-k}}} \tag{2}$$

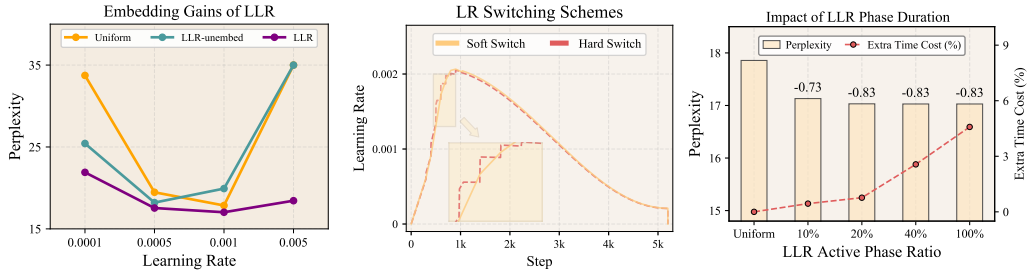


Figure 4: **Left:** Embedding gains of `LLR` compared to baselines across different LRs with LLaMa-135M. "LLR-unembed" denotes the ablation variant without the tailored spectral-based adjustment for Embedding layer; **Middle:** Illustration of hard (perplexity = 17.18) versus soft (perplexity = 17.03) LR switching schemes with LLaMa-135M; **Right:** Impact of `LLR` phase duration on perplexity and extra time cost. The computation time for `Uniform` is 4.51 H100 hours.

**Algorithm 1:** `LLR`

**Require:** Global LR $\eta$, number of training steps $t_{max}$, interval $\tilde{t}$ of using `LLR`, maximum scaling ratio $s$, switching steps $t_{switch}$, and $\alpha_T^i$ refers to $i_{th}$ layer's `PL_Alpha_Hill` at update step $T \in \{0, \tilde{t}, 2\tilde{t}, ..., t_{max}\}$

**for** $t \leftarrow 0$ *to* $t_{max}$ **do**
  **if** $mod(t, \tilde{t}) = 0$ **then**
    **Step 1:** Compute $\alpha_T^i$ for all layers using fomula (2);
    **Step 2:** Calculate the target global LR $f_T(i)$ using $\alpha_T^i$ and scaling function (3) bounded by $\eta$ and $s\eta$;
    **Step 3 (Soft Switch):** Linearly transition layer $i$'s LR from its current value to $f_T^{t+t_{switch}}(i)$ over the next $t_{switch}$ steps to avoid spikes;
    **Step 4:** Follow the cosine decay scheduler with global LR $f_T(i)$ starting from $f_T^{t+t_{switch}}(i)$ until $t + \tilde{t}$;

where the parameter $k$ controls the lower cutoff in the fitting process. In all experiments, we set $k = \frac{n}{2}$, thereby estimating the slope using the largest half of the eigenvalues (Detailed study of PL fitting method refer to Appendix D, Figure 8).

### 2.2 Layerwise Learning Rate for LLMs (LLR)

Based on the `PL_Alpha_Hill` characteristics in Section 2.1, we propose a Layerwise LR (`LLR`) allocation method. `LLR` calculates the `PL_Alpha_Hill` values of all layers, assigning larger LRs to those with higher values and smaller LRs to those with lower values (see Figure 3). The mapping from `PL_Alpha_Hill` values to per-layer LRs follows the bounded scaling function:

$$f_T(i) = \eta \cdot \left(\frac{\alpha_T^i - \alpha_T^{\min}}{\alpha_T^{\max} - \alpha_T^{\min}}(s-1) + 1\right) \tag{3}$$

where $\eta$ is the global LR, and $(1, s)$ define the range of scaling ratios applied to $\eta$. $\alpha_T^i$ is the `PL_Alpha_Hill` value of layer $i$ at step $T \in \{0, \tilde{t}, 2\tilde{t}, ..., t_{max}\}$, with $\tilde{t}$ denotes the interval for calculating `PL_Alpha_Hill` and $t_{max}$ the total training steps. While $\alpha_T^{min}$ and $\alpha_T^{max}$ are the minimum and maximum `PL_Alpha_Hill` values among all layers at step $T$. Formula (3) guarantees that the adjusted global LR, $f_T(i)$, remains within $[\eta, s\eta]$ as a scaled variant of $\eta$. Let $\eta^t$ and $f_T^t(i)$ denote the LRs at step $t \in \{0, 1, 2, ..., t_{max}\}$ under a cosine decay scheduler, corresponding to the global learning rate $\eta$ and the layer-wise value $f_T(i)$, respectively.

To effectively adapt the HT-SR theory to LLMs, we introduce three tailored designs targeting the unique characteristics of Transformer architectures:

**Tailored Embedding Treatment.** Considering the `Embedding` (and `Output_Head`) layer's persistently high `PL_Alpha_Hill` values across all training stages (refer to Figure 2 **(Left)** and Fig-

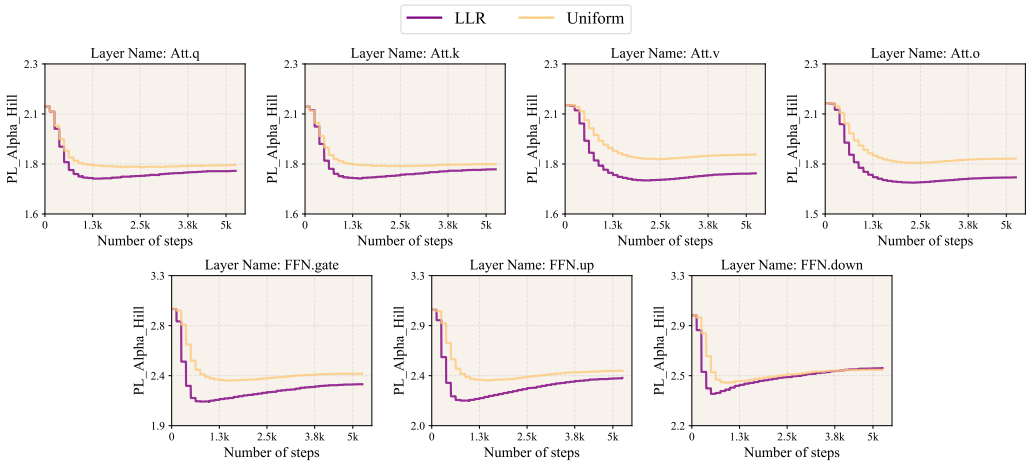


Figure 5: Evolution of `PL_Alpha_Hill` for different parameter groups when training LLaMA-135M with `LLR` (perplexity = 17.03) and `Uniform` (perplexity = 17.86). The curves are computed every 100 training steps.

ure 12 of Appendix E), we fix its LR at the scaling function's upper bound $s\eta$, following Wang et al. (2025). This design is crucial to prevent the under-adaptation of the scaling function (Formula 3) that would otherwise occur. Figure 4 **(Left)** validates this approach: our tailored strategy yields significant performance gains compared to the **"LLR-unembed"** variant, ensuring that these critical layers receive sufficient updates.

**Soft Layer-wise LR Switch.** Traditional methods typically employ a **"Hard Switch"** that instantaneously shifts the LR $\eta^t$ to a target value $f_T^t(i)$, often causing detrimental **"LR spikes"** (as visualized in the red dashed line in Figure 4 (**Middle**)). To mitigate this, we propose a Soft Switch mechanism. Instead of an abrupt change, we linearly increase the current LR $\eta^t$ over a window of $t_{switch} \leq \tilde{t}$ steps towards the target LR $f_T^{t+t_{switch}}(i)$ calculated at step $t + t_{switch}$. This "look-ahead" smoothing strategy eliminates spikes, thereby enhancing training stability. In our implementation, we set $t_{switch} = 0.5\tilde{t} = 50$ (approximately 2.6M tokens) by default (Detailed study refer to Appendix D, Figure 9).

**Efficient Active Phase.** We observe that the layer-wise `PL_Alpha_Hill` statistics tend to stabilize after processing approximately the first 20% of training tokens (as shown in Figure 5). Based on this finding, we restrict the computationally expensive layer-wise LR updates to this initial 20% phase. Figure 4 **(Right)** demonstrates that this strategy maintains comparable performance to full-time updates while drastically reducing computational overhead, making `LLR` highly efficient for large-scale pre-training.

We provide the details of `LLR` in Algorithm 1. By appropriately constraining dominant components, `LLR` establishes an adaptive and robust framework for layerwise LR allocation in LLM training.

### 2.3 Layer-wise PL_Alpha_Hill Dynamics

In this section, we investigate how `LLR` influences the optimization dynamics of different parameter groups, we analyze the evolution of the `PL_Alpha_Hill` in LLaMA-135M. Figure 5 shows the `PL_Alpha_Hill` for each major parameter group when training with `LLR` (perplexity = 17.03) and `Uniform` (perplexity = 17.86). We compute `PL_Alpha_Hill` every 100 update steps. Several trends are evident from the figure.❶ The `Attention` parameters (`Att.q`, `Att.k`, `Att.v`, `Att.o`) consistently exhibit smaller `PL_Alpha_Hill`, whereas the `FFN` parameters (`FFN.gate`, `FFN.up`, `FFN.down`) maintain larger `PL_Alpha_Hill` throughout training. ❷ The `PL_Alpha_Hill` of all parameter groups change substantially during the early phase of training (approximately the first 20% of update steps). This pronounced variation highlights the importance of periodically updating the layer-wise LRs, rather than keeping them fixed over time. ❸ Compared with `Uniform`, `LLR` markedly reduces the `PL_Alpha_Hill` across all parameter groups. This reduction correlates with the improved perplexity achieved by `LLR`, suggesting that better control of `PL_Alpha_Hill` contributes directly to the enhanced training performance.

Table 1: Hyperparameters used in pre-training experiments. LLR-$s$ denotes the $(1, s)$ parameter setting in LLR.

| Model Size | Tokens | LARS-LR/WD | LAMB-LR/WD | Sharpness-LR/WD | AdamW/LLR-LR/WD | LLR-$s$ |
|---|---|---|---|---|---|---|
| 60M | 1.5B | 0.001/1e-6 | 0.05/0.1 | 0.0005/0.1 | 0.001/0.1 | 5 |
| 135M | 3B | 0.001/1e-6 | 0.05/0.1 | 0.0001/0.1 | 0.001/0.1 | 5 |
| 350M | 7B | 0.001/1e-6 | 0.01/0.1 | 0.0001/0.1 | 0.001/0.1 | 5 |
| 1B | 20B | 0.001/1e-6 | 0.01/0.1 | 0.0001/0.1 | 0.0005/0.1 | 5 |

For more detailed analysis of PL_Alpha_Hill about LLR and Uniform, refer to Appendix E.

## 3 Empirical results

In this section, we begin by presenting the complete experimental setup (Section 3.1), followed by a comparison between LLR and several baselines (Section 3.2). Finally, we demonstrate the effectiveness of LLR across diverse model architectures, and various optimizers.

### 3.1 Experimental setup

**Models and Datasets**. We perform a comprehensive experimental study encompassing pre-training, zero-shot evaluation, and fine-tuning over a diverse range of model architectures and parameter scales. **(i) Pre-training.** Models are pre-trained on the FineWeb dataset (Penedo et al., 2024) under Chinchilla scaling law Hoffmann et al. (2022). We evaluate two categories of models: LLaMa-based architectures (60M, 135M, 350M, and 1B) and the GPT-nano architecture (135M) (Table 8 in Appendix B). This design supports systematic evaluation of scalability and architectural generalization. **(ii) Zero-shot Commonsense Reasoning Evaluation.** Following pre-training, we evaluate the emergent reasoning capabilities of the LLaMa-1B checkpoints. This is conducted via zero-shot inference on a comprehensive benchmark suite of seven unseen commonsense reasoning tasks: PIQA (Bisk et al., 2020), SIQA (Sap et al., 2019), HellaSwag (Zellers et al., 2019), WinoGrande Sakaguchi et al. (2021), ARC-c (Clark et al., 2018), ARC-e (Clark et al., 2018), and OBQA (Mihaylov et al., 2018). The evaluation utilizes the standard prompts provided by the lm-evaluation-harness to quantify out-of-data performance. **(iii) Fine-tuning.** We fine-tune RoBERTa-base (Liu et al., 2019) on the Commonsense Reasoning benchmark (Hu et al., 2023) (Table 6 in Appendix B), which comprises the seven downstream tasks described above, enabling a direct comparison under a parameter-efficient adaptation setting.

**Baselines.** We compare with four representative methods: (i) Uniform: Based on standard AdamW (Loshchilov & Hutter, 2017) or Muon (Liu et al., 2025) optimizers, applies the same learning rate to all layers without any layer-wise differentiation; (ii) LARS (You et al., 2017): A first-moment-based optimizer that assigns per-layer learning rates proportional to the ratio of weight to gradient norms; (iii) LAMB (You et al., 2019): A second-moment-based adaptive optimization algorithm that scales learning rates in a layer-wise manner according to weight norms to ensure training stability; (iv) Sharpness (Wang et al., 2025): Determines a fixed learning rate ratio across different layers via grid search based on sharpness information, without providing an automatic adjustment mechanism.

**Hyperparameters.** The detailed hyperparameter settings for all model sizes are summarized in Table 1 and Table 9-12 in Section C. All models are trained with gradient clipping at 1.0 and a cosine learning rate schedule, with 10% of the training tokens used for learning rate warmup. We conduct grid search over learning rates $\{0.00001, 0.00005, 0.0001, 0.0005, 0.001, 0.005\}$ as shown in Figure 1. The best configuration for each scale are reported in the Table the corresponding $(1, s)$ parameter settings are also detailed in the tables. LLR is performed every 5.2M tokens (100 update steps) throughout all experiments (Detailed study refer to Appendix D, Figure 9).

### 3.2 LLM Pre-training

In this section, we present the experimental results for LLR and all baselines across optimizers (AdamW and Muon), and parameter scales (60M–1B), followed by a comprehensive comparison between Uniform and LLR.

Table 2: **(Main result).** Comparison with LLR and all baselines on pre-training various sizes of LLaMa models on FineWeb dataset. Validation perplexity (↓) is reported.

| Model Size | Uniform | LARS (You et al., 2017) | LAMB (You et al., 2019) | Sharpness (Wang et al., 2025) | LLR |
|---|---|---|---|---|---|
| 60M | 21.94 | 52.52 | 23.53 | 23.28 | **20.30** |
| 135M | 17.86 | 32.78 | 18.59 | 18.54 | **17.03** |
| 350M | 12.96 | 19.04 | 14.56 | 14.91 | **12.71** |
| 1B | 9.77 | 11.81 | 10.68 | 9.77 | **9.59** |

Table 3: **(Zero-shot results of commonsense-reasoning tasks in Tabel 2).** Zero-shot evaluation results (↑) on seven commonsense reasoning benchmarks using the LLaMa-1B model pretrained with different methods.

| Method | OBQA | winogrande | ARC-c | ARC-e | Hellaswag | SIQA | PIQA | Avg. |
|---|---|---|---|---|---|---|---|---|
| Uniform | 28.0 | 55.01 | 30.72 | 66.50 | 39.29 | 40.38 | 69.75 | 47.09 |
| LARS | 24.0 | 52.25 | 27.05 | 58.71 | 33.36 | 38.18 | 67.36 | 42.99 |
| LAMB | 24.6 | 50.59 | 29.27 | 62.37 | 36.45 | 39.30 | 68.01 | 44.37 |
| Sharpness | 26.0 | 53.59 | 30.80 | 67.72 | 39.36 | 40.89 | 70.40 | 46.97 |
| LLR | **29.6** | **56.67** | **34.64** | **70.46** | **40.53** | **40.79** | **70.46** | **49.02** |

### 3.2.1 Main Results

Table 2 presents the main results of our study, where we evaluate the effectiveness of LLR and all baselines on the pre-training of LLaMa models with varying parameter scales (60M, 135M, 350M, and 1B) on the FineWeb dataset.

**Observations in Table 2. ❶ Superior and consistent gains across all baselines.** Across all evaluated model sizes, LLR surpasses both the Uniform baseline and the adaptive learning rate methods (LARS, LAMB, Sharpness). This consistent superiority over baselines demonstrates our approach's robustness for LLM pre-training. **❷ Scalability to Larger Models.** The superiority of LLR is consistently observed from the smallest (60M) to the largest (1B) LLaMa models, achieving performance gains even at the billion-parameter scale. This consistency underscores the scalability and general applicability of our method in large-scale language model pre-training.

Furthermore, our experiments reveal that existing methods, originally designed for architectures without Attention components, such as LARS and LAMB, do not yield optimal results for LLMs. This may be attributed to their lack of consideration for the distinct characteristics and optimization requirements of Attention and FFN layers within transformer architectures. In contrast, our approach demonstrate that a tailored Layerwise LR allocation method can consistently enhance LLM training by explicitly accounting for the heterogeneous characteristics of different layers.

**Zero-shot Results in Table 3.** We evaluate the pretrained LLaMa-1B models, based on the checkpoints obtained from the pretraining experiments in Table 2, on 7 zero-shot commonsense reasoning tasks with lm-eval-harness under its default prompt configuration. As shown in Table 3, LLR achieves the best performance on all 7 benchmarks, boosting average accuracy from 47.09% to 49.02%. This confirms that pretraining gains effectively transfer to downstream reasoning tasks.

### 3.2.2 More benefits from LLR

LLR demonstrates that **" one LR doesn't fit all "** and provides a substantial acceleration in training.

**Performance of uniform LR at the scaling upper bound.** Table 4 presents the validation perplexity of different model sizes using AdamW optimizers with a uniform LR across all layers set to match the maximum Layerwise LR (upper bound) determined by LLR. Compared with the results in Table 2 and Table 4, LLR consistently outperforms both the upper bound and lower bound of uniform LR scaling across different optimizers and model sizes.

Table 4: **(Up bound of LR scaling).** Validation perplexity (↓) of AdamW with a uniform LR equal to $s$ times that in Uniform of Table 2, matching the maximum LR from LLR's scaling method.

| Model Size | 60M | 135M | 350M | 1B |
|---|---|---|---|---|
| LR (Upbound) | 0.005 | 0.005 | 0.005 | 0.0025 |
| Uniform-Upbound | 68.28 | 70.81 | 56.96 | 30.56 |
| LLR | **20.30** | **17.03** | **12.71** | **9.59** |

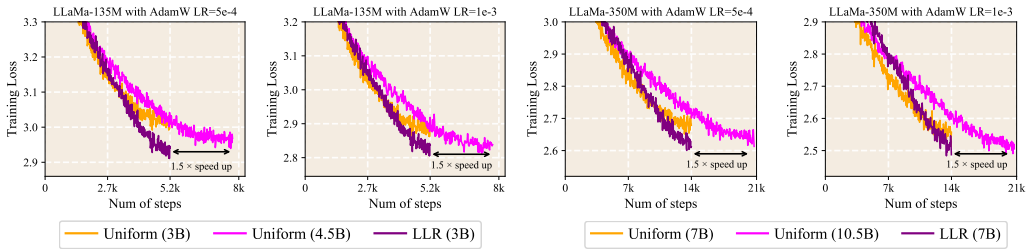


Figure 6: Training loss for the LLaMa-135M and LLaMa-350M model, comparing `Uniform` (3B/7B and 4.5B/10.5B tokens) against `LLR` (3B/7B tokens). The experiments employ AdamW under two different learning rates.

***These findings confirm that a uniform LR configuration is inherently suboptimal***, whereas the proposed layer-wise LR strategy enables a more effective utilization of the capabilities of different optimizers.

**Speedup.** Figure 6 presents the training loss curves for LLaMa-135M and LLaMa-350M model during pre-training, comparing `LLR` with `Uniform` across two learning rates. Across all configurations, `LLR` consistently achieves lower training loss with 3B/7B tokens compared to `Uniform` with the same number of training tokens, highlighting its effectiveness in accelerating convergence. Furthermore, `LLR` attains performance comparable to or better than that of `Uniform` at 4.5B/10.5B tokens, corresponding to an approximate 1.5× speedup.

### 3.3 More Analysis

In this section, we evaluate `LLR` across more model architecture and optimizer to demonstrate its generality and robustness.

**Results with Muon Optimizer.** We investigate whether the proposed `LLR` can consistently improve performance when paired with optimizers beyond AdamW. Specifically, Table 5 presents results on various LLaMa model sizes trained with the Muon optimizer on the FineWeb dataset. Across all model scales, `LLR` delivers lower validation perplexity than `Uniform`, indicating that our method complements alternative optimizers like Muon, as its benefits stem from the spectral characteristics of the weight matrices rather than specific algorithmic mechanics.

Table 5: **(Pretraining with Muon).** Performance comparison on various sizes of LLaMa models trained with the Muon optimizer on the FineWeb. Validation perplexity (↓) is reported. The reported LR is {LR for Muon part} and the {LR for AdamW part} is is one-tenth of {LR for Muon part}.

| | LLaMa-60M | | LLaMa-135M | |
|---|---|---|---|---|
| LR | Uniform | LLR | Uniform | LLR |
| 0.05 | 20.02 | **19.76** | 19.94 | **19.24** |
| 0.01 | 19.49 | **17.70** | 16.51 | **16.29** |
| 0.005 | 21.07 | **19.03** | 16.97 | **16.00** |

## 4 Conclusion

We introduced `LLR`, a layer-wise learning rate adjustment strategy that leverages `PL_Alpha_Hill` during LLM training. Across diverse setups, including different model architectures, multiple optimizers, and varying parameter scales, `LLR` consistently delivers lower perplexity and better downstream performance than existing baselines, while maintaining robustness to variations in training configurations. Moreover, `LLR` accelerates convergence by up to 1.5× across multiple optimizers. More importantly, it inherits near-optimal learning rate settings from standard uniform LR, minimizing tuning overhead and enabling easy integration into existing pipelines. These results suggest that `LLR` is an effective and broadly applicable optimization technique for LLM training.

**Limitations.** This work does not investigate the applicability of `LLR` to multimodal tasks, such as image-to-text or text-to-image generation, where optimization dynamics may differ substantially.

## REFERENCES

Jeff Alstott, Ed Bullmore, and Dietmar Plenz. powerlaw: a python package for analysis of heavy-tailed distributions. *PloS one*, 9(1):e85777, 2014.

Jimmy Ba, Murat A Erdogdu, Taiji Suzuki, Zhichao Wang, Denny Wu, and Greg Yang. High-dimensional asymptotics of feature learning: How one gradient step improves the representation. *Advances in Neural Information Processing Systems*, 35:37932–37946, 2022.

Yonatan Bisk, Rowan Zellers, Jianfeng Gao, Yejin Choi, et al. Piqa: Reasoning about physical commonsense in natural language. In *Proceedings of the AAAI conference on artificial intelligence*, volume 34, pp. 7432–7439, 2020.

Peter Clark, Isaac Cowhey, Oren Etzioni, Tushar Khot, Ashish Sabharwal, Carissa Schoenick, and Oyvind Tafjord. Think you have solved question answering? try arc, the ai2 reasoning challenge. *arXiv preprint arXiv:1803.05457*, 2018.

Aaron Clauset, Cosma Rohilla Shalizi, and Mark EJ Newman. Power-law distributions in empirical data. *SIAM review*, 51(4):661–703, 2009.

Romain Couillet and Zhenyu Liao. *Random matrix methods for machine learning*. Cambridge University Press, 2022.

Soufiane Hayou and Liyuan Liu. Optimal embedding learning rate in llms: The effect of vocabulary size. *arXiv preprint arXiv:2506.15025*, 2025.

Di He, Ajay Jaiswal, Songjun Tu, Li Shen, Ganzhao Yuan, Shiwei Liu, and Lu Yin. Alphadecay: Module-wise weight decay for heavy-tailed balancing in llms. *arXiv preprint arXiv:2506.14562*, 2025.

Jordan Hoffmann, Sebastian Borgeaud, Arthur Mensch, Elena Buchatskaya, Trevor Cai, Eliza Rutherford, Diego de Las Casas, Lisa Anne Hendricks, Johannes Welbl, Aidan Clark, et al. Training compute-optimal large language models. *arXiv preprint arXiv:2203.15556*, 2022.

Zhiqiang Hu, Lei Wang, Yihuai Lan, Wanyu Xu, Ee-Peng Lim, Lidong Bing, Xing Xu, Soujanya Poria, and Roy Ka-Wei Lee. Llm-adapters: An adapter family for parameter-efficient fine-tuning of large language models. *arXiv preprint arXiv:2304.01933*, 2023.

Vignesh Kothapalli, Tianyu Pang, Shenyang Deng, Zongmin Liu, and Yaoqing Yang. From spikes to heavy tails: Unveiling the spectral evolution of neural networks. *Transactions on Machine Learning Research*, 2025.

Yann LeCun, Yoshua Bengio, and Geoffrey Hinton. Deep learning. *nature*, 521(7553):436–444, 2015.

Jingyuan Liu, Jianlin Su, Xingcheng Yao, Zhejun Jiang, Guokun Lai, Yulun Du, Yidao Qin, Weixin Xu, Enzhe Lu, Junjie Yan, et al. Muon is scalable for llm training. *arXiv preprint arXiv:2502.16982*, 2025.

Yinhan Liu, Myle Ott, Naman Goyal, Jingfei Du, Mandar Joshi, Danqi Chen, Omer Levy, Mike Lewis, Luke Zettlemoyer, and Veselin Stoyanov. Roberta: A robustly optimized bert pretraining approach. *arXiv preprint arXiv:1907.11692*, 2019.

Zihang Liu, Yuanzhe Hu, Tianyu Pang, Yefan Zhou, Pu Ren, and Yaoqing Yang. Model balancing helps low-data training and fine-tuning. *arXiv preprint arXiv:2410.12178*, 2024.

Ilya Loshchilov and Frank Hutter. Decoupled weight decay regularization. *arXiv preprint arXiv:1711.05101*, 2017.

Haiquan Lu, Yefan Zhou, Shiwei Liu, Zhangyang Wang, Michael W Mahoney, and Yaoqing Yang. Alphapruning: Using heavy-tailed self regularization theory for improved layer-wise pruning of large language models. *Advances in Neural Information Processing Systems*, 37:9117–9152, 2024.

Michael Mahoney and Charles Martin. Traditional and heavy tailed self regularization in neural network models. In *International Conference on Machine Learning*, pp. 4284–4293. PMLR, 2019.

Charles H Martin and Michael W Mahoney. Traditional and heavy-tailed self regularization in neural network models. *arXiv preprint arXiv:1901.08276*, 2019.

Charles H Martin, Tongsu Peng, and Michael W Mahoney. Predicting trends in the quality of state-of-the-art neural networks without access to training or testing data. *Nature Communications*, 12 (1):4122, 2021.

Todor Mihaylov, Peter Clark, Tushar Khot, and Ashish Sabharwal. Can a suit of armor conduct electricity? a new dataset for open book question answering. *arXiv preprint arXiv:1809.02789*, 2018.

Long Ouyang, Jeffrey Wu, Xu Jiang, Diogo Almeida, Carroll Wainwright, Pamela Mishkin, Chong Zhang, Sandhini Agarwal, Katarina Slama, Alex Ray, et al. Training language models to follow instructions with human feedback. *Advances in neural information processing systems*, 35: 27730–27744, 2022.

Rui Pan, Xiang Liu, Shizhe Diao, Renjie Pi, Jipeng Zhang, Chi Han, and Tong Zhang. Lisa: Layerwise importance sampling for memory-efficient large language model fine-tuning. *Advances in Neural Information Processing Systems*, 37:57018–57049, 2024.

Guilherme Penedo, Hynek Kydlíček, Loubna Ben allal, Anton Lozhkov, Margaret Mitchell, Colin Raffel, Leandro Von Werra, and Thomas Wolf. The fineweb datasets: Decanting the web for the finest text data at scale, 2024. URL `https://arxiv.org/abs/2406.17557`.

Alec Radford, Karthik Narasimhan, Tim Salimans, Ilya Sutskever, et al. Improving language understanding by generative pre-training. 2018.

Keisuke Sakaguchi, Ronan Le Bras, Chandra Bhagavatula, and Yejin Choi. Winogrande: An adversarial winograd schema challenge at scale. *Communications of the ACM*, 64(9):99–106, 2021.

Maarten Sap, Hannah Rashkin, Derek Chen, Ronan LeBras, and Yejin Choi. Socialiqa: Commonsense reasoning about social interactions. *arXiv preprint arXiv:1904.09728*, 2019.

Ashish Vaswani, Noam Shazeer, Niki Parmar, Jakob Uszkoreit, Llion Jones, Aidan N Gomez, Łukasz Kaiser, and Illia Polosukhin. Attention is all you need. *Advances in neural information processing systems*, 30, 2017.

Jinbo Wang, Mingze Wang, Zhanpeng Zhou, Junchi Yan, Lei Wu, et al. The sharpness disparity principle in transformers for accelerating language model pre-training. *arXiv preprint arXiv:2502.19002*, 2025.

Jason Wei, Xuezhi Wang, Dale Schuurmans, Maarten Bosma, Fei Xia, Ed Chi, Quoc V Le, Denny Zhou, et al. Chain-of-thought prompting elicits reasoning in large language models. *Advances in neural information processing systems*, 35:24824–24837, 2022.

Yaoqing Yang, Ryan Theisen, Liam Hodgkinson, Joseph E Gonzalez, Kannan Ramchandran, Charles H Martin, and Michael W Mahoney. Test accuracy vs. generalization gap: Model selection in nlp without accessing training or testing data. In *Proceedings of the 29th ACM SIGKDD Conference on Knowledge Discovery and Data Mining*, pp. 3011–3021, 2023.

Yang You, Igor Gitman, and Boris Ginsburg. Large batch training of convolutional networks. *arXiv preprint arXiv:1708.03888*, 2017.

Yang You, Jing Li, Sashank Reddi, Jonathan Hseu, Sanjiv Kumar, Srinadh Bhojanapalli, Xiaodan Song, James Demmel, Kurt Keutzer, and Cho-Jui Hsieh. Large batch optimization for deep learning: Training bert in 76 minutes. *arXiv preprint arXiv:1904.00962*, 2019.

Rowan Zellers, Ari Holtzman, Yonatan Bisk, Ali Farhadi, and Yejin Choi. Hellaswag: Can a machine really finish your sentence? *arXiv preprint arXiv:1905.07830*, 2019.

Yushun Zhang, Congliang Chen, Tian Ding, Ziniu Li, Ruoyu Sun, and Zhiquan Luo. Why transformers need adam: A hessian perspective. *Advances in neural information processing systems*, 37:131786–131823, 2024a.

Yushun Zhang, Congliang Chen, Ziniu Li, Tian Ding, Chenwei Wu, Diederik P Kingma, Yinyu Ye, Zhi-Quan Luo, and Ruoyu Sun. Adam-mini: Use fewer learning rates to gain more. *arXiv preprint arXiv:2406.16793*, 2024b.

Yefan Zhou, Tianyu Pang, Keqin Liu, Michael W Mahoney, Yaoqing Yang, et al. Temperature balancing, layer-wise weight analysis, and neural network training. *Advances in Neural Information Processing Systems*, 36:63542–63572, 2023.

## A Related Work

**Layerwise Learning Rate.** Although a uniform LR is the standard in deep network training, recent work has investigated layerwise LR allocation to improve optimization efficiency (Pan et al., 2024; Zhang et al., 2024b). LARS (You et al., 2017) and LAMB (You et al., 2019) scale LRs by the gradient-to-weight norm ratio, but as they were not designed for LLMs, they provide only marginal gains and demand additional tuning. Wang et al. (2025) introduced a blockwise LR allocation method that leverages sharpness disparities to accelerate pretraining, though it relies on exhaustive grid search. Complementarily, Hayou & Liu (2025) observed a dependence of optimal embedding-layer LRs on vocabulary size, suggesting distinct scaling rules across components. The closest related work is TempBalance (Zhou et al., 2023), which adapts HT-SR to adjust learning rates at the layer level for improved optimization. However, its applicability is restricted to CNNs and fine-tuning scenarios with limited data volume.

**HT-SR theory for LLM**. HT-SR theory describes a statistical phenomenon in which the weights of well-trained neural networks exhibit strong correlations, giving rise to heavy-tailed patterns in the ESD of Layerwise weight matrices (Mahoney & Martin, 2019; Martin et al., 2021). Empirical evidence shows that, across various stages of training—whether at the early, intermediate, or final phase—different components of LLMs (`Embed`, `Attention`, `FFN`) display distinct heavy-tailed structures in their ESDs (Couillet & Liao, 2022; Kothapalli et al., 2025; Ba et al., 2022). Building on this observation, numerous studies have sought to balance these heavy-tailed characteristics through applications of HT-SR, including model selection (Mahoney & Martin, 2019; Martin et al., 2021; Yang et al., 2023), module-wise adaptive training (Zhou et al., 2023), LLM pruning (Lu et al., 2024), and module-wise weight-decay allocation (He et al., 2025), achieving notable improvements in large-scale model training. However, it remains unclear if HT-SR can be utilized for layerwise LR designing for LLM pre-training.

## B Finetuning Results, More Baselines' Results and GPT-nano Results

**Finetuning Results.** We evaluate all methods on finetuning tasks using `roberta-base` from the Commonsense Reasoning dataset. As shown in Table 6, `LLR` achieves the best performance on 6/7 tasks. These results demonstrate that `LLR` is not only effective in the pretraining stage but also generalizes well to finetuning scenarios.

Table 6: **(Finetuning tasks).** Finetuning results on seven benchmarks from the Commonsense Reasoning dataset using `roberta-base` with different methods.

| Method | OBQA | Winogrande | ARC-c | ARC-e | Hellaswag | SIQA | PIQA | Avg. |
|---|---|---|---|---|---|---|---|---|
| `Untuned` | 16.0 | 48.61 | 22.52 | 26.34 | 23.52 | 35.05 | 50.54 | 31.80 |
| `Uniform` | 22.6 | 49.88 | 24.57 | 25.76 | 24.37 | 35.41 | 50.27 | 33.27 |
| `LARS` | 19.4 | 50.12 | 23.63 | 27.02 | 24.63 | 33.73 | 49.56 | 32.58 |
| `LAMB` | 16.0 | 48.62 | 23.12 | 26.68 | 23.14 | 36.08 | 50.05 | 31.96 |
| `Sharpness` | 21.8 | 49.01 | 23.21 | **25.13** | 24.25 | 35.47 | 51.03 | 32.84 |
| `LLR` | **23.6** | **51.30** | **24.59** | 25.21 | **24.92** | **36.24** | **51.20** | **33.86** |

Table 7: Performance comparison with HT-SR based methods. We compare `LLR` against `Alphadecay` (He et al. (2025)) and `Tempbalance` (Zhou et al. (2023)) across 60M and 135M parameter scales.

| Method | `Uniform` | `Alphadecay` | `Tempbalance` | `LLR` |
|---|---|---|---|---|
| 60M | 21.92 | 21.58 | 21.54 | 20.3 |
| 135M | 17.86 | 17.35 | 17.19 | 17.03 |

**More Baselines' Results.** To isolate the contribution of our LLM-specific architectural designs, we benchmark `LLR` against two other approaches rooted in the same HT-SR theory: `Alphadecay` He et al. (2025), which applies HT-SR to modulate weight decay, and `Tempbalance` Zhou et al. (2023), which targets acceleration for simpler architectures like ResNet. As presented in Table 7, `LLR` achieves significantly lower perplexity compared to both baselines across different model scales

(60M and 135M). This performance gap is instructive: while `Alphadecay` and `Tempbalance` share the theoretical underpinnings, they lack the tailored adaptations for the Transformer architecture. These results empirically validate our hypothesis that the specific designs introduced in Figure 4 **(e.g., [Tailored regularization for embedding layers, Soft layer-wise LR switch])** are essential for effectively translating the HT-SR theory into the LLM regime.

Table 8: **(GPT-nano Evaluation).** Performance comparison of `LLR` and all baselines on GPT-nano trained on the FineWeb dataset. Validation perplexity (↓) is reported.

| Method | `Uniform` | `LARS` | `LAMB` | `Sharpness` | `LLR` |
|---|---|---|---|---|---|
| Perplexity | 22.16 | 31.59 | 74.24 | 24.28 | **20.53** |

**Results of GPT-nano.** We evaluate the proposed `LLR` on GPT-nano, as shown in Table 8. The comparison includes `LARS`, `LAMB`, `Sharpness`, `Uniform` (AdamW), and `LLR`. The results demonstrate that `LLR` achieves the lowest validation perplexity, significantly outperforming all baseline methods. This further confirms the robustness and broad applicability of our approach across different model architectures.

## C Details of Experiments

This section provides detailed configurations for both pretraining and finetuning experiments. In Table 9 and Table 10, we present the architectural parameters of LLaMa models and the learning rate and weight decay settings for different methods of Nano-GPT.

Table 9: Hyperparameters of LLaMa models used in this paper.

| LLaMa-Size | Hidden | Intermediate | Heads | Layers | Steps | Data amount | Batch Size | Sequence Length |
|---|---|---|---|---|---|---|---|---|
| 60M | 768 | 2048 | 6 | 6 | 10K | 1.5B | 512 | 1024 |
| 135M | 768 | 2048 | 12 | 12 | 20K | 3B | 512 | 1024 |
| 350M | 1024 | 2736 | 16 | 24 | 60K | 7B | 512 | 1024 |
| 1B | 2048 | 5461 | 32 | 24 | 100K | 20B | 512 | 1024 |

Table 10: Learning Rate and Weight Decay used for different methods in pretraining GPT-nano on FineWeb dataset.

| Method | `Uniform` | `LARS` | `LAMB` | `Sharpness` | `LLR` |
|---|---|---|---|---|---|
| Learning Rate | 1e-3 | 5e-3 | 5e-2 | 1e-4 | 1e-3 |
| Weight Decay | 0.1 | 1e-6 | 0.1 | 0.1 | 0.1 |

In Table 11 and Table 12, we describe the model and dataset parameters used for finetuning roberta-base on the Commonsense Reasoning Benchmark and the corresponding learning rate and weight decay settings.

Table 11: Hyperparameters used of all methods for finetuning roberta-base on the Commonsense Reasoning Benchmark.

| Model name | Hidden | Intermediate | Heads | Layers |
|---|---|---|---|---|
| Roberta-base | 12 | 3072 | 12 | 12 |
| Train Samples | Test Samples | Batch Size | Max_length | Training Epoch |
| 170K | 22.4K | 64 | 512 | 1 |

Table 13: **(Dependent t-test results on FineWeb with LLaMA-135M using the AdamW optimizer).** Each method is evaluated over six repeated experiments with random seeds {5, 6, 7, 8, 9, 10}, and compared against LLR using a dependent t-test. Perplexity is reported as mean ± standard deviation. The resulting p-values correspond to comparisons with LLR.

| Method | Uniform | LARS | LAMB | Sharpness | LLR |
|---|---|---|---|---|---|
| Perplexity | 17.79 (± 0.05) | 17.07 (±0.04) | 33.06 (±0.42) | 18.58 (±0.15) | 18.84 (±0.25) |
| P-value | 1.0e-10 | 1.9e-9 | 6.3e-7 | 9.3e-6 | |

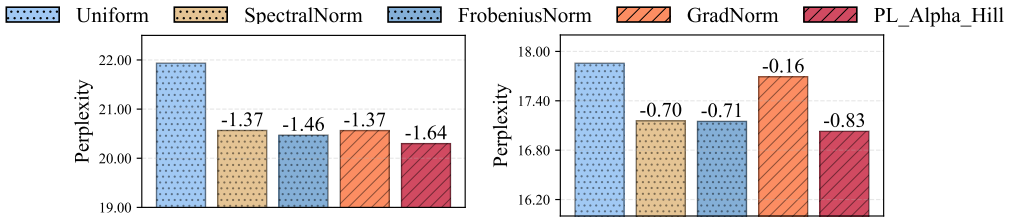


(a) LLaMa-60M (b) LLaMa-135M

Figure 7: **(Varying HT-SR metrics).** Comparing PL_Alpha_Hill with multiple metrics under different learning rate settings. The value on the top of each bar indicates the difference from the leftmost bar in each plot and the same processing is applied in Figure 8, Figure 9 and Figure 10.

Table 12: Learning Rate and Weight Decay used for different methods in finetuning Roberta-based on the Commonsense Reasoning Benchmark.

| Method | Uniform | LARS | LAMB | Sharpness | LLR |
|---|---|---|---|---|---|
| Learning Rate | 1e-4 | 5e-5 | 1e-4 | 1e-5 | 1e-4 |
| Weight Decay | 0.1 | 1e-6 | 0.1 | 0.1 | 0.1 |

## D Ablation Experiments

This section presents ablation experiments evaluating the effects of different LR scheduling strategies, metrics, and related factors. We begin with repeated experiments across multiple random seeds (Table 13), with statistical validation via dependent t-tests. Figure 7 compares scheduling metrics, analyzing validation perplexity. Figure 8 examines the impact of different PL fitting methods on model performance. Figure 9 investigates the impact of varying PL fitting gaps on model performance. Figures 10 investigate the effects of varying the $(1, s)$ hyperparameter in LLR.

**Repeat Experiments.** Table 13 provides a comparison of several LR scheduling strategies, evaluated through repeated experiments with different random seeds. The dependent t-test results further substantiate these findings, with statistically significant p-values supporting the superiority of LLR over all other optimizers.

**Varying HT-SR metrics.** To investigate the effect of different learning rate scheduling metrics on model performance, we conducted ablation studies comparing these methods with LLaMa-60M and LLaMa-135M. While prior work has primarily explored Uniform scheduling and GradNorm as representative metrics, our study additionally evaluates PL_Alpha_Hill, FrobeniusNorm, and SpectralNorm under identical training settings. Results in Figure 7 show that, PL_Alpha_Hill consistently achieves the lowest validation perplexity (lower is better), highlighting its effectiveness over other evaluated metrics.

**Varying PL fitting methods.** In our proposed framework, the HT-SR metric PL_Alpha_Hill is derived through PL fitting, and the choice of fitting method can affect final training effectiveness. To assess this impact, we evaluate Goodness-of-fit (Alstott et al., 2014; Martin et al., 2021; Clauset et al., 2009), Fix-finger (Yang et al., 2023), and Median (Zhou et al., 2023) under identical experimental conditions in Figure 8. Across all tested experiments, Median maintains

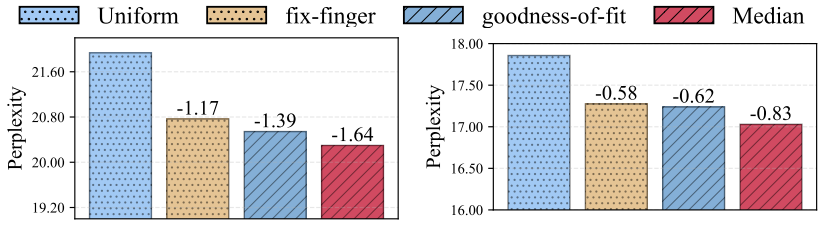


(a) LLaMa-60M (b) LLaMa-135M

Figure 8: **(Varying PL fitting methods).** Analysis of three PL fitting methods—`Goodness-of-fit`, `Fix-finger`, and `Median`—across LLaMa-60M and LLaMa-135M.

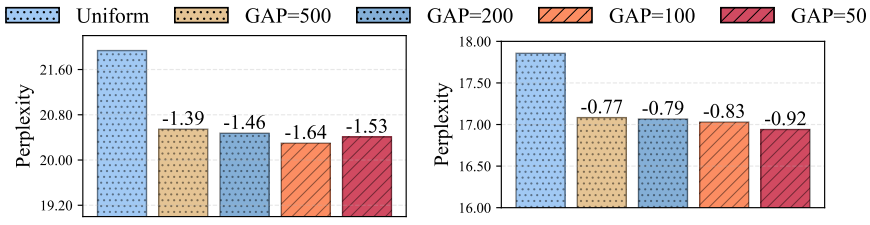


(a) LLaMa-60M (b) LLaMa-135M

Figure 9: **(Varying PL fitting gaps).** PL fitting is conducted at varying gaps across training steps to evaluate the trade-off between performance. Bars represent validation perplexity (lower is better).

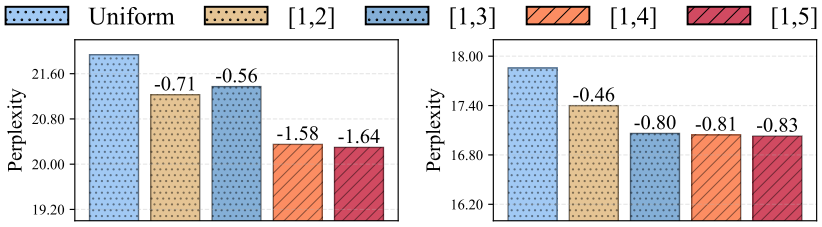


(a) LLaMa-60M (b) LLaMa-135M

Figure 10: **(Hyperparameter study on $(1, s)$).** Results of a hyperparameter search for $(1, s)$ across LLaMa-60M and LLaMa-135M on the FineWeb dataset. The bar plots display validation perplexity (lower is better).

competitive or superior training performance compared to the other two approaches, making it the preferred choice for PL fitting within our method.

**Varying PL fitting gaps.** To evaluate the effect of PL fitting frequency on model performance, we compare different update gaps under identical experimental conditions in Figure 9. Across all tests, our method achieves stable performance across all gap settings, consistently outperforming the uniform baseline. Even when the fitting interval is as large as 500 training steps, the method maintains competitive perplexity, demonstrating robustness. These results justify using a larger fitting gap in practice to balance performance and cost.

**Hyperparameter study on $(1, s)$.** Figure 10 demonstrates that `LLR`, with $(1, s)$ settings of (1, 2), (1, 3), (1, 4) and (1, 5), consistently surpasses the `Uniform` baseline across all experiments, with stable gains across schedules, highlighting its robustness and insensitivity to reasonable variations in $s$.

## E SPECTRAL FEATURE ANALYSIS OF LLR

To understand the structural impact of our proposed method on the model weights, we analyze the ESD plot of the layer-wise correlation matrices. Figure 11 presents a comparative visualization of the spectral distributions for the LLaMa-135M model trained with `LLR` versus the Uniform baseline.

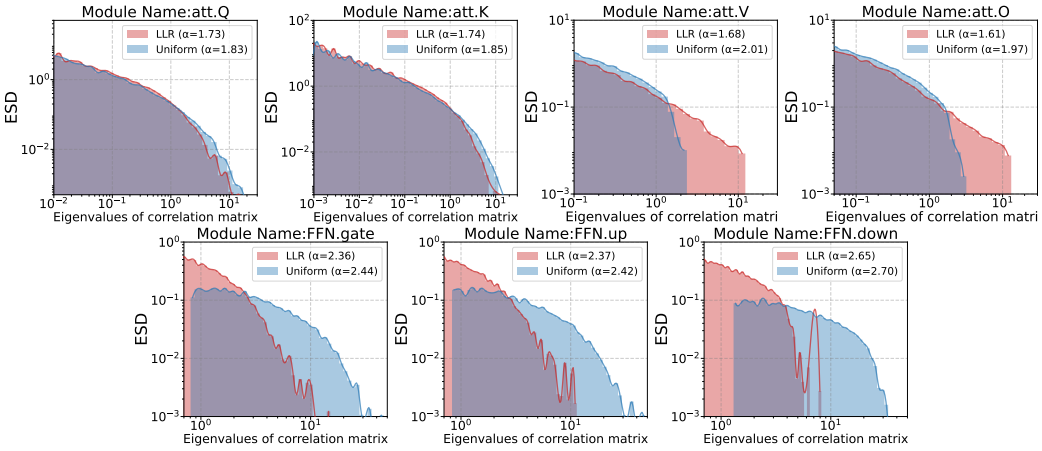


Figure 11: Comparison of ESD distributions across layers of LLaMa-135M under different training methods (`LLR`: Perplexity=17.03 vs. Uniform: Perplexity=17.86). Attention-related layers (e.g., att.q, att.k) exhibit notably heavier spectral tails in contrast to FFN-associated layers. Our method systematically balances the heavy-tailed properties across layers by appropriately configuring layer-wise LR, thereby enhancing overall model performance.

The plots illustrate the distribution of eigenvalues on a log-log scale, where the slope of the tail relates to the PL exponent $\alpha$. A smaller $\alpha$ indicates a "heavier" tail, which is theoretically associated with better generalization capabilities in deep networks.

Comparing the two methods, we observe distinct spectral behaviors:

- **Layer Heterogeneity:** Attention-related layers (e.g., `att.Q`, `att.K`) naturally exhibit heavier tails compared to FFN layers, suggesting different intrinsic regularization needs.
- **Effect of LLR:** The `LLR` method (shown in red) systematically shifts the spectral distributions compared to the Uniform baseline (shown in blue). For instance, in the `att.V` layer, `LLR` results in a heavier tail ($\alpha = 1.68$) compared to Uniform ($\alpha = 2.01$).

This modulation of spectral shapes demonstrates that `LLR` does not merely scale the weights but fundamentally alters the optimization trajectory, leading to a weight configuration that generalizes better (Perplexity: 17.03) than the Uniform approach (Perplexity: 17.86).

We further examine the evolution of spectral features across different components during the pre-training phase.

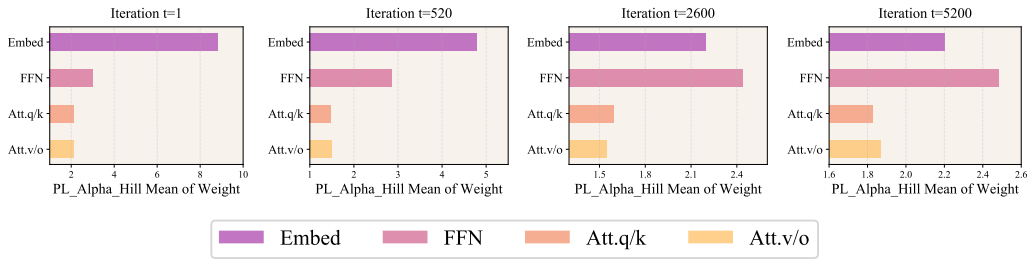


Figure 12: Evolution of `PL_Alpha_Hill` distributions from weights of LLaMA-135M components across iterations during pre-training on the Fineweb dataset, trained by AdamW with uniform LR.

As illustrated in Figure 12, there is a significant heterogeneity in the PL_Alpha_Hill values among different layers. Specifically, attention-related components (e.g., Att.q/k, Att.v/o) consistently exhibit lower PL_Alpha_Hill values compared to FFN layers and Embeddings throughout the training iterations (from $t = 1$ to $t = 5200$). This persistent disparity indicates that different components have distinct capacities and learning dynamics, thereby justifying the necessity of the LLR strategy to assign layer-specific learning rates rather than a uniform global learning rate.